atmosphere

Article

The Dynamic Impacts of COVID-19 Pandemic Lockdown on the Multifractal Cross-Correlations between $PM_{2.5}$ and O_3 Concentrations in and around Shanghai, China

Xing Li * and Fang Su

School of Finance, Shanghai University of Finance and Economics, Shanghai 200433, China
* Correspondence: xingli@163.sufe.edu.cn

Abstract: Although the outbreak of the COVID-19 pandemic caused serious restrictions on human activities in and around Shanghai, China, the period can be viewed as a helpful experiment to investigate the correlation between $PM_{2.5}$ and O_3 concentrations. In this study, the hourly $PM_{2.5}$ and O_3 series in four cities (i.e., Shanghai, Jiaxing, Nantong and Suzhou) from 27 November 2019 to 23 March 2020 are used. The "seesaw effect" is observed in the study data. The dynamic impacts of the COVID-19 pandemic on the multifractal cross-correlations and the coordinated control degree of $PM_{2.5}$-O_3 are examined in these cities. First of all, the multifractal cross-correlations, multifractality components and dynamic influences of the COVID-19 pandemic on cross-correlations between $PM_{2.5}$ and O_3 in four cities are illustrated. Furthermore, a new quantification index, ζ, evaluating the coordinated control degree of $PM_{2.5}$-O_3 is developed, validated and compared. The multifractal cross-correlation analysis results reveal that the cross-correlations between $PM_{2.5}$ and O_3 in and around Shanghai both before and during the COVID-19 partial lockdown have multifractal characteristics. Moreover, there are weaker multifractal cross-correlation degrees of $PM_{2.5}$-O_3 in four cities during the COVID-19 partial lockdown. The multifractal cause analysis based on stochastic simulation illustrates that the impacts of multifractality due to the nonlinear correlation part are greater than the linear correlation part and the fat-tailed probability distribution part in and around Shanghai. The intrinsic multifractal cross-correlations decreased in all cities during the COVID-19 lockdown. However, the effects of the COVID-19 lockdown on the multifractal cross-correlations are limited from the perspective of intrinsic multifractality. The mean values of ζ in and around Shanghai all increase during the COVID-19 partial lockdown, which indicates that the $PM_{2.5}$-O_3 coordinated control degrees in all four cities become weaker.

Keywords: COVID-19 lockdown; $PM_{2.5}$; O_3; MF-DCCA; multifractal cause analysis; coordinated control degree

check for updates

Citation: Li, X.; Su, F. The Dynamic Impacts of COVID-19 Pandemic Lockdown on the Multifractal Cross-Correlations between $PM_{2.5}$ and O_3 Concentrations in and around Shanghai, China. *Atmosphere* **2022**, *13*, 1964. https://doi.org/10.3390/atmos13121964

Academic Editor: László Bencs

Received: 19 October 2022
Accepted: 21 November 2022
Published: 24 November 2022

1. Introduction

In December 2019, several cases of unusual pneumonia were identified in Wuhan, China. The disease, known as COVID-19, spreads rapidly after the outbreak. The central and local authorities in China enforced a partial lockdown to contain the spread of the virus. With the lockdown, almost all industrial activities and mass transportation were restricted. Although the outbreak of the COVID-19 pandemic caused serious restrictions on human activities in and around Shanghai, China, the period can be viewed as a helpful experiment to investigate the correlation between $PM_{2.5}$ and O_3 concentrations.

Aiming to alleviate serious air pollution problems, the Chinese authority implemented the "Atmospheric Pollution Prevention and Control Action Plan" from 2013 to 2017. During this period, the $PM_{2.5}$ concentrations declined by 30–40%, while O_3 concentrations rose by 8.75–10%, which is a "seesaw effect" between $PM_{2.5}$ and O_3, i.e., an increase of O_3 following a decrease of $PM_{2.5}$ [1,2]. Several studies have discussed the complex correlation between $PM_{2.5}$ and O_3 [3–5].

Analyzing the fractal features of air quality series is generally a complex task. Therefore, various nonlinear methods have been utilized to capture these phenomena. Of these methods, detrended fluctuation analysis (DFA) [6] proposed by Peng et al., is capable of studying the long-range power law correlation analysis of non-stationary time series. Based on DFA, Kantelhardt et al. [7] developed the multifractal detrended fluctuation analysis (MF-DFA), which can accurately quantify the long-range correlation of non-stationary time series. The MF-DFA has been successfully used in studying the evolution of air pollutants [8–12]. Wang [13] used the MF-DFA method to analyze the multifractal characteristics of polluted time series in Beijing, Zhengzhou and Jinan. Li [14] employed the MF-DFA method to investigate the impacts of the COVID-19 pandemic on the multifractality of air quality index time series in Shanghai. Zhang et al. [15] used the MF-DFA method to explore the cross-correlations between $PM_{2.5}$ concentration and climatic conditions. Zhang et al. [16] utilized the MF-DFA method to discuss the multifractal characteristics of $PM_{2.5}$ and O_3 concentrations. Moreover, multifractal detrended cross-correlation analysis (MF-DCCA) [17] is an efficient method in terms of analyzing two spatially or temporally correlated time series and detecting the long-range power-law cross-correlation of considered signals of non-stationarity. Xu et al. [18] employed the MF-DCCA method to prove that the cross-correlations between O_3 and its precursors NO_x have multifractal features and long-term persistence. Wu et al. [2] utilized the MF-DCCA method to illustrate the multifractal cross-correlation between $PM_{2.5}$ and O_3.

However, there are no empirical studies on the impact of the COVID-19 pandemic on multifractal cross-correlations of $PM_{2.5}$-O_3. Accordingly, in this study, the apparent and intrinsic multifractal cross-correlations between $PM_{2.5}$ and O_3 concentrations in and around Shanghai, China, are determined and compared before and during the COVID-19 partial lockdown. Furthermore, the coordinated control degrees of $PM_{2.5}$-O_3 are analyzed and examined before and during the COVID-19 partial lockdown in four cities (i.e., Shanghai, Jiaxing, Nantong and Suzhou).

This paper is organized as follows: The data description and data preprocessing methods are described in Section 2. The MF-DCCA method, analysis of the multifractal causes based on the stochastic simulation method and a new quantification index of coordinated control degree of $PM_{2.5}$-O_3 are introduced in Section 3. The multifractal cross-correlation analysis, multifractality components, the coordinated control degrees of $PM_{2.5}$-O_3 in four cities and the dynamic impacts of the COVID-19 pandemic are illustrated in Section 4. Finally, this study is summarized in Section 5.

2. Data Description and Preprocessing Method

To analyze the dynamic impacts of the COVID-19 pandemic on multifractal cross-correlations between $PM_{2.5}$ and O_3, the hourly $PM_{2.5}$ and O_3 concentrations in and around Shanghai, China, (including Shanghai, Jiaxing, Nantong and Suzhou) are obtained from RESSET Air Quality Monitoring Big Data Platform (http://res.resset.com/AQM, accessed on 27 October 2021) which are collected from the Ministry of Ecology and Environment of the People's Republic of China (http://english.mee.gov.cn/, accessed on 27 October 2021) The daily $PM_{2.5}$ and O_3 concentrations in these cities are collected from the Air Quality Publishing Platform of China (http://www.aqistudy.cn/historydata/index.php, accessed on 27 October 2021).

The study data are from 27 November 2019 to 23 March 2020. The total number is 22,656. Considering the period of Shanghai public health emergency level I, the data from 25 January 2020 to 23 March 2020 is defined as the period during the COVID-19 partial lockdown and the data from 27 November 2019 to 24 January 2020 is chosen as before the COVID-19 partial lockdown. Due to monitoring instrument calibration and maintenance, the number of missing and outlier data is 798, 3.5% of the total data. In this paper, arithmetic mean is adopted to handle these abnormal data based on the daily $PM_{2.5}$ and O_3 series.

The hourly $PM_{2.5}$ and O_3 series before and during the COVID-19 partial lockdown are illustrated in Figure 1 and the descriptive statistics are listed in Table 1. Compared to the period before the COVID-19 lockdown, the increase percentages of O_3 are 84.2% (Shanghai), 68.9% (Nantong) and 130.8% (Suzhou), while the decrease percentage of $PM_{2.5}$ are 33.2% (Shanghai), 12.9% (Nantong) and 34.0% (Suzhou) during the COVID-19 lockdown. It can be observed that the blue lines representing the mean of $PM_{2.5}$ descend, while the blue lines representing the mean of O_3 ascend during the COVID-19 lockdown in Shanghai, Nantong and Suzhou in Figure 1. It is shown that there is an increase of O_3 following the decrease of $PM_{2.5}$, i.e., a "seesaw effect" between $PM_{2.5}$ and O_3. The values of skewness and kurtosis in Table 1 are significantly different from zero. The results indicate that the $PM_{2.5}$ and O_3 pollutants do not follow a normal distribution. It is necessary to study the relationship between the $PM_{2.5}$ and O_3 by nonlinear methods.

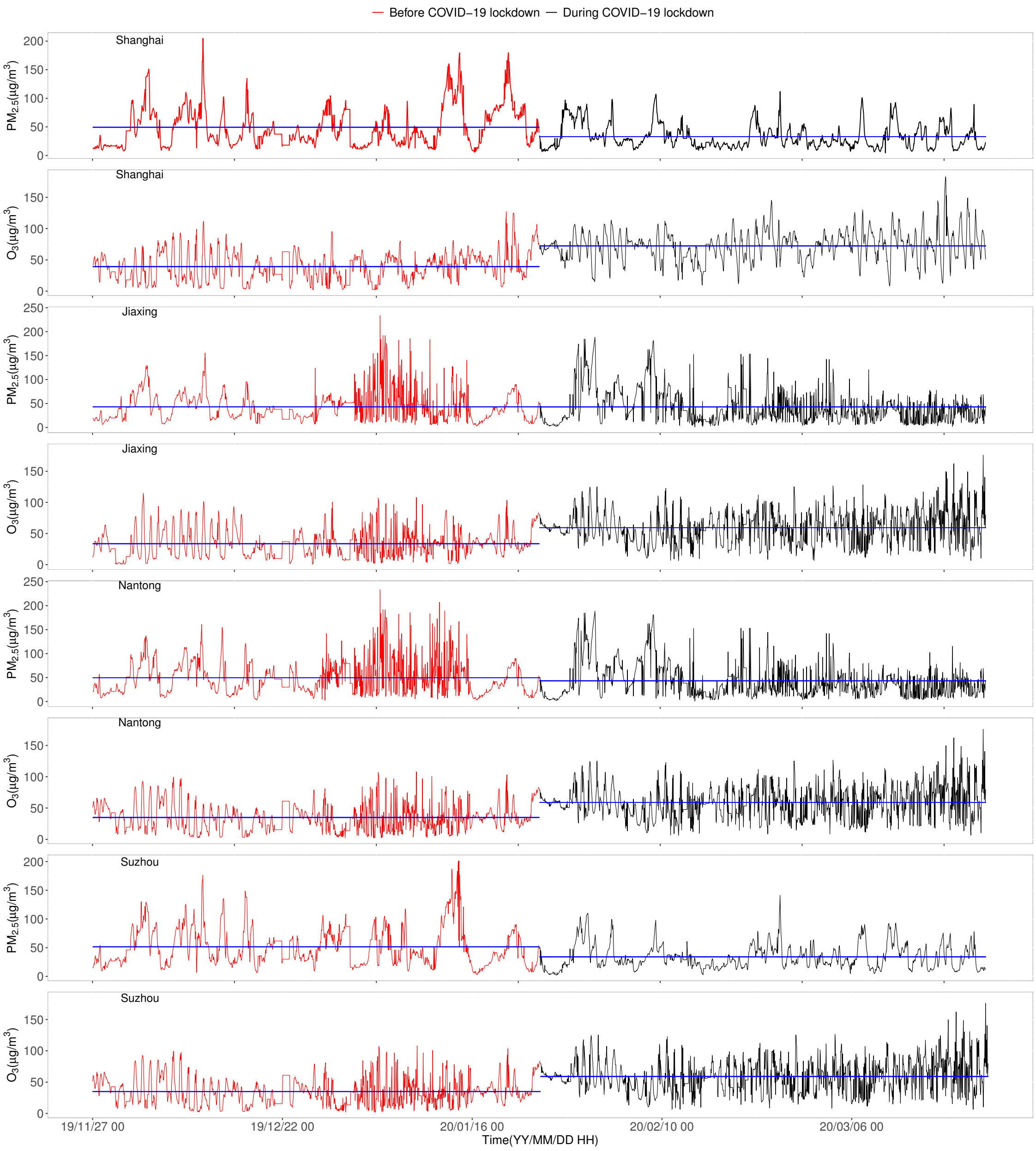

Figure 1. The hourly $PM_{2.5}$ and O_3 series in Shanghai, Jiaxing, Nantong and Suzhou before and during the COVID-19 partial lockdown, the blue line is the mean value of $PM_{2.5}$ and O_3 in different period in four cities.

Table 1. Descriptive statistics of the hourly $PM_{2.5}$ and O_3 series in Shanghai, Jiaxing, Nantong and Suzhou before and during the COVID-19 partial lockdown.

City	Pollutant	Mean			Std.		Median		Skewness		Kurtosis	
		Period I(A)	Period II(B)	Ratio (B-A)/A	Period I	Period II	Period I	Period II	Period I	Period II	Period I	Period II
Shanghai	$PM_{2.5}$ (μg/m^3)	49.26	32.89	−33.2%	34.75	21.07	39.75	27.15	1.19	1.18	1.28	0.76
	O_3 (μg/m^3)	39.26	72.33	84.2%	22.73	24.07	38.37	73.58	0.52	0.23	0.16	0.98
Jiaxing	$PM_{2.5}$ (μg/m^3)	42.99	42.87	−0.3%	30.75	35.99	37.19	32.7	1.62	1.51	3.92	2.24
	O_3 (μg/m^3)	33.58	59.34	76.7%	22.04	25.73	31	58.22	0.87	0.45	0.43	0.25
Nantong	$PM_{2.5}$ (μg/m^3)	49.62	43.2	−12.9%	34.92	35.81	43.12	33.6	1.26	1.51	2.02	2.29
	O_3 (μg/m^3)	34.93	58.99	68.9%	21.24	25.3	32.66	57.59	0.72	0.46	0.13	0.25
Suzhou	$PM_{2.5}$ (μg/m^3)	51.49	33.99	−34.0%	33.86	21.31	42.62	28.85	1.1	1.11	1.25	1.23
	O_3 (μg/m^3)	29.42	67.9	130.8%	21.95	26.19	26.06	67.12	0.92	0.38	0.58	0.4

To compare the multifractality of the different series, the logarithmic values are calculated and utilized in this research.

3. Methodology

3.1. Mf-Dcca Method

In this study, $PM_{2.5}$ and O_3 time series are defined as $\{x_i\} = \{x_1, x_2, \cdots, x_N\}$ and $\{y_i\} = \{y_1, y_2, \cdots, y_N\}$ with the same length N, respectively; the MF-DCCA method can be described as in following steps.

(1) Calculate the profiles of $\{x_i\}$ and $\{y_i\}$:

$$X_i = \sum_{k=1}^{i}(x_k - \bar{x}),\ i = 1, \cdots, N, Y_i = \sum_{k=1}^{i}(y_k - \bar{y}),\ i = 1, \cdots, N, \tag{1}$$

where $\bar{x} = \frac{1}{N}\sum_{i=1}^{N} x_i$ and $\bar{y} = \frac{1}{N}\sum_{i=1}^{N} y_i$.

(2) The profile is divided into $N_s = \mathrm{int}(N/s)$ non-overlapping bins with length s. Since N is not a multiple of s, a short part of the series may be left. In order to include this part, the same procedure is repeated starting from the opposite end, obtaining a total of $2N_s$ bins.

(3) For each bin, the least square linear fit is performed and the cross-correlation for each box is given by

$$Var_s^v = \left\{\frac{1}{s}\sum_{i=1}^{s}[X_i^v - \tilde{X}_i^v]^2 \times [Y_i^v - \tilde{Y}_i^v]^2\right\}^{q/4} \tag{2}$$

where $\tilde{X}_i^v$ and $\tilde{Y}_i^v$ is the fitting polynomial in segment v.

(4) The qth order fluctuation function is obtained by:

$$F_{x/y}(q,s) = \begin{cases} \left\{\frac{1}{2N_s}\sum_{v=1}^{2N_s}(Var_s^v)\right\}^{1/q}, & \text{if } q \neq 0. \\ \frac{1}{2}\left[F_{x/y}(1,s) + F_{x/y}(-1,s)\right], & \text{if } q = 0. \end{cases} \tag{3}$$

where this q-order can take any real value. In this study, q varies from -5 to 5. Steps (2) to (4) can be repeated by varying the values of s.

(5) If the series are long-range power-law correlated, the generalized Hurst exponent $H_{x/y}(q)$ will show power-law behavior:

$$F_{x/y}(q,s) \approx s^{H_{x/y}(q)}. \tag{4}$$

If $H_{x/y}(q)$ is independent of q, the cross-correlations between the time series are monofractal. If $H_{x/y}(q)$ is dependent on q, the cross-correlations between the time series are multifractal. The range of $H_{x/y}(q)$, $\Delta H_{x/y} = H_{x/y}(\min(q)) - H_{x/y}(\max(q))$, indicates the extent of cross-correlation. The scaling exponent $\tau_{x/y}(q)$ is expressed as:

$$\tau_{x/y}(q) = qH_{x/y}(q) - 1 \tag{5}$$

The singularity strength $\alpha_{x/y}$ and the multifractal spectrum $f_{x/y}(\alpha)$ can be calculated with the following equations:

$$\alpha_{x/y} = \frac{d\tau_{x/y}q}{dq} = H_{x/y}(q) + qH'_{x/y}(q) \tag{6}$$

according to the definition, $\alpha_{x/y}$ can be any real value.

$$f_{x/y}(\alpha_{x/y}) = q\alpha_{x/y} - \tau_{x/y}(q) = 1 + q[\alpha_{x/y} - H_{x/y}(q)] \tag{7}$$

The multifractal spectrum width, $\Delta\alpha_{x/y} = \max(\alpha_{x/y}) - \min(\alpha_{x/y})$, represents the degree of the multifractal cross-correlation.

3.2. Multifractal Cause Analysis

Traditionally, there are two types of multifractality in time series: fat tails and/or the long-range temporal correlations [7]. Recent studies present that the multifractality in time series may originate from long-range nonlinear autocorrelations, the presence of fat tails in probability distributions of data or linear autocorrelations present in shorter (finite) time series [19]. However, many studies illustrate that the time series generated from monofractal models and mathematical models can produce spurious multifractality [20,21]. The linear correlations or long memory in time series is not sufficient for the emergence of multifractality [22]. The nonlinear correlations are the genuine source of the multifractality [23,24]. Whether the empirical multifractality is intrinsic or apparent and the origin of the measured multifractality in time series are critical problems that have attracted many researchers' attention [14,19,23–26].

In order to determine different sources of apparent multifractal cross-correlations, the width of the original series' multifractal spectrum $\Delta\alpha_{x/y}$ includes the nonlinear correlation part $\Delta\alpha^{NL}_{x/y}$, the linear correlation part $\Delta\alpha^{LM}_{x/y}$ and the fat-tailed probability distribution part $\Delta\alpha^{PDF}_{x/y}$ can be expressed as the following equation [14,26,27]:

$$\Delta\alpha_{x/y} = \Delta\alpha^{NL}_{x/y} + \Delta\alpha^{LM}_{x/y} + \Delta\alpha^{PDF}_{x/y}. \tag{8}$$

Furthermore, the shuffling procedure and the Fourier transform surrogate procedure are applied to decompose different parts of apparent multifractality. The improved, amplitude adjusted Fourier transform (IAAFT) algorithm [28] is employed in the surrogate procedure. A more practical and convenient way, which is directly introducing linear correlations into random time series generated from the original time series, has been employed to construct the surrogate time series in this study. By construction, The width of the multifractal spectrum of the surrogate series can reflect the multifractality degree of the linear correlation part and the fat-tailed probability distribution part [29]. The specific formulas of the three parts can be qualified as follows.

$$\Delta\alpha^{PDF}_{x/y} = \Delta\alpha^{shuf}_{x/y}. \tag{9}$$

$$\Delta\alpha^{LM}_{x/y} = \Delta\alpha^{surr}_{x/y} - \Delta\alpha^{PDF}_{x/y}. \tag{10}$$

$$\Delta\alpha^{NL}_{x/y} = \Delta\alpha_{x/y} - \Delta\alpha^{surr}_{x/y}. \tag{11}$$

The intrinsic multifractality $\Delta\alpha_{x/y}^{INTR}$ can be expressed as

$$\Delta\alpha_{x/y}^{INTR} = \Delta\alpha_{x/y}^{NL}. \tag{12}$$

According to Equation (11), the intrinsic multifractality can also be expressed as:

$$\Delta\alpha_{x/y}^{INTR} = \Delta\alpha_{x/y} - \Delta\alpha_{x/y}^{surr}. \tag{13}$$

The ratio of the intrinsic multifractality to apparent multifractality can be expressed as

$$\text{INTR ratio}_{x/y} = \Delta\alpha_{x/y}^{INTR} / \Delta\alpha_{x/y}. \tag{14}$$

Further to studies in [14], multifractal cause analysis based on the stochastic simulation (MCASS) method applied in this study, are as follows:

Step 1 The original series is shuffled to remove any potential correlations. The MF-DCCA analysis is conducted on the shuffled series and the multifractal characteristic $H_{x/y}^{shuf}(q), \Delta\alpha_{x/y}^{shuf}$ is determined.

Step 2 The surrogate series are constructed by phase-randomizing the original series using the IAAFT algorithm. The MF-DCCA analysis is carried out on the surrogate series and $H_{x/y}^{surr}(q), \Delta\alpha_{x/y}^{surr}$ are calculated;

Step 3 Steps 1–2 are repeated until 80,000 sets of $\{H_{x/y}^{shuf}(q), H_{x/y}^{surr}(q), \Delta\alpha_{x/y}^{shuf}, \Delta\alpha_{x/y}^{surr}\}$ of the hourly $PM_{2.5}$ and O_3 series in and around Shanghai, China, before and during the COVID-19 partial lockdown are accumulated.

Step 4 The differences between $H_{x/y}^{shuf}(q), H_{x/y}^{surr}(q), \Delta\alpha_{x/y}^{shuf}, \Delta\alpha_{x/y}^{surr}$ are checked to determine the components of the multifractality and intrinsic multifractality of the hourly $PM_{2.5}$ and O_3 series in four cities before and during the COVID-19 partial lockdown, respectively.

Step 5 Finally, the comparisons between the above multifractality parameters are applied to determine the dynamic impacts of the COVID-19 pandemic on the intrinsic multifractality hourly $PM_{2.5}$ and O_3 series in and around Shanghai, China.

3.3. Formation of a New Index ζ

Further to Section 3.2, the multifractal cross-correlations between the original series can be decomposed into three parts: nonlinear correlations, linear correlations and fat-tailed probability distribution. The nonlinear correlations are the genuine source of the multifractality [23,24], indicating the apparent multifractal cross-correlation may be larger than or equal to the intrinsic multifractality part. Here, we develop a new index to qualify the $PM_{2.5}$-O_3 coordinated control degree based on intrinsic multifractality and this index is an extension of the work of Wu et al. [2]. By contrast, the analysis of multifractal sources in the paper of Wu et al. [2] is still the traditional method and the η introduced by Wu et al. did not consider the difference between apparent multifractality and intrinsic multifractality. Furthermore, the 10,000 simulations utilized in the MCASS method can give a more robust result.

The new index is defined as

$$\zeta = \frac{\text{INTR ratio}_{x/y}}{\sqrt{\sigma_x \sigma_y}}. \tag{15}$$

where, $\sigma_x^2 = \frac{1}{N}\sum_{i=1}^{N}(x-\bar{x})^2, \sigma_y^2 = \frac{1}{N}\sum_{i=1}^{N}(y-\bar{y})^2$.

To evaluate the capability of the above index, two extreme scenarios need to be analyzed. Scenario I, $PM_{2.5}$ and O_3 have not been controlled cooperatively at all. In this scenario, the concentration values of one pollutant which is completely controlled remain almost constant ($\sigma \to 0$). However, the other pollutant is not controlled at all, which means its concentration values are in extreme fluctuation ($\sigma \neq 0$). Based on Equation (15), $\zeta \to \infty$. Scenario II, $PM_{2.5}$ and O_3 are completely coordinated controlled, which means, there is little temporal fluctuation in the cross-correlations between $PM_{2.5}$ and O_3 series. This case implies a lack of the intrinsic multifractal cross-correlations of $PM_{2.5}$-O_3. So INTR $\text{ratio}_{x/y} \to 0$ and $\zeta \to 0$ based on Equation (15).

All in all, the index ζ can be utilized as a quantification index of the $PM_{2.5}$-O_3 coordinated control degree of different cities. The smaller the ζ value, the greater the $PM_{2.5}$-O_3 coordinated control degree. The bigger the ζ value, the weaker the $PM_{2.5}$-O_3 coordinated control degree.

4. Results and Discussion

4.1. Multifractal Cross-Correlations of $PM_{2.5}$-O_3

To analyze the cross-correlation relationship between hourly $PM_{2.5}$ and O_3 series in and around Shanghai before and during the COVID-19 partial lockdown quantitatively, the MF-DCCA method is applied to calculate the generalized Hurst exponents and the multifractal spectra. The results are illustrated in Figures 2 and 3.

Figure 2 shows that $H^{SH}_{x/y,bl}(q)$, $H^{SH}_{x/y,dl}(q)$, $H^{JX}_{x/y,bl}(q)$, $H^{JX}_{x/y,dl}(q)$, $H^{NT}_{x/y,bl}(q)$, $H^{NT}_{x/y,dl}(q)$, $H^{SZ}_{x/y,bl}(q)$ and $H^{SZ}_{x/y,dl}(q)$ depend on q, which implies that the cross-correlations between hourly $PM_{2.5}$ and O_3 series in and around Shanghai both before and during the COVID-19 partial lockdown are multifractal. $H^{SH}_{x/y,bl}(2) = 0.873$, $H^{SH}_{x/y,dl}(2) = 0.761$, $H^{JX}_{x/y,bl}(2) = 0.822$, $H^{JX}_{x/y,dl}(2) = 0.913$, $H^{NT}_{x/y,bl}(2) = 0.887$, $H^{NT}_{x/y,dl}(2) = 0.925$, $H^{SZ}_{x/y,bl}(2) = 0.855$ and $H^{SZ}_{x/y,dl}(2) = 0.844$. $H^{SH}_{x/y,dl}(2) < H^{SH}_{x/y,bl}(2)$ indicate there is weaker multifractal cross-correlation between $PM_{2.5}$ and O_3 in Shanghai during the COVID-19 partial lockdown. Figure 3 shows that $\Delta\alpha^{SH}_{x/y,bl} < \Delta\alpha^{SH}_{x/y,dl}$, $\Delta\alpha^{JX}_{x/y,bl} < \Delta\alpha^{JX}_{x/y,dl}$, $\Delta\alpha^{NT}_{x/y,bl} < \Delta\alpha^{NT}_{x/y,dl}$ and $\Delta\alpha^{SZ}_{x/y,bl} < \Delta\alpha^{SZ}_{x/y,dl}$, which demonstrate there are weaker multifractal cross-correlation degrees between $PM_{2.5}$ and O_3 in four cities during the COVID-19 partial lockdown.

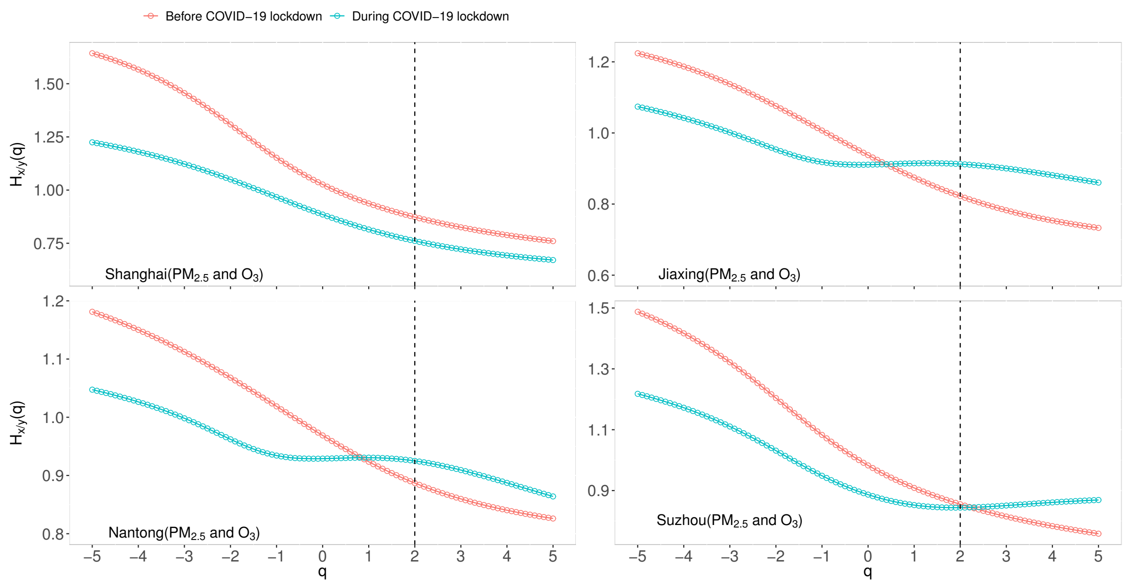

Figure 2. The q dependences of the generalized Hurst exponents $H_{x/y}(q)$ in and around Shanghai before and during the COVID-19 partial lockdown. q and $H_{x/y}(q)$ are defined in Equations (3) and (4).

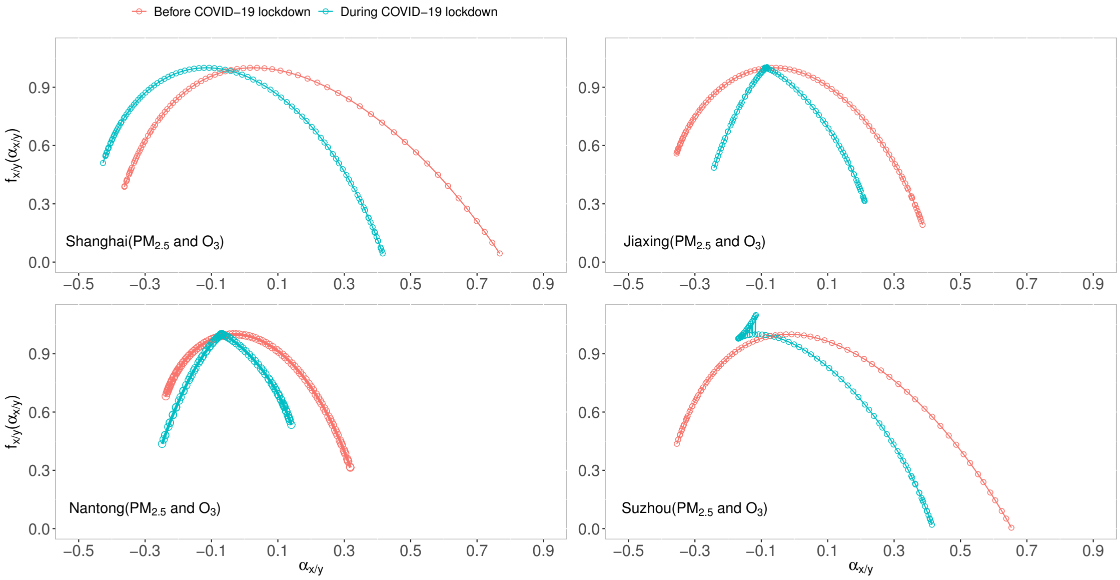

Figure 3. The multifractal spectra $(\alpha_{x/y}, f_{x/y}(\alpha_{x/y}))$ in and around Shanghai before and during the COVID-19 partial lockdown. $\alpha_{x/y}$ and $f_{x/y}(\alpha_{x/y})$ are defined in Equations (6) and (7).

4.2. Causes of Cross-Correlations between $PM_{2.5}$ and O_3

After shuffling and phase-randomizing the original $PM_{2.5}$ and O_3 in and around Shanghai before and during the COVID-19 partial lockdown 10,000 times, respectively, the MCASS method is employed on these series. The generalized Hurst exponents $H_{x/y}(q)$ between the shuffled and the surrogate $PM_{2.5}$ and O_3 in four cities before and during the COVID-19 partial lockdown are illustrated in Figure 4. The generalized Hurst exponent in Shanghai $H^{SH,shuf}_{x/y,bl}(q)$ and $H^{SH,shuf}_{x/y,dl}(q)$ depend on q which shows that the cross-correlations between the shuffled time series are multifractal; $H^{SH,ori}_{x/y,bl}(q) > H^{SH,shuf}_{x/y,bl}(q)$, $H^{SH,ori}_{x/y,dl}(q) > H^{SH,shuf}_{x/y,dl}(q)$ show that the degrees of multifractal cross-correlations between original series are always bigger than that between shuffled series for a given q. Moreover, the generalized Hurst exponent in Shanghai $H^{SH,surr}_{x/y,bl}(q)$ and $H^{SH,surr}_{x/y,dl}(q)$ depending on q shows that the cross-correlations between the surrogate series are multifractal and the discrepancies between original and surrogate time series $H^{SH,ori}_{x/y,bl}(q)$ and $H^{SH,surr}_{x/y,bl}(q)$, $H^{SH,ori}_{x/y,dl}(q)$ and $H^{SH,surr}_{x/y,dl}(q)$ are not substantial, respectively. Similar conclusions can be observed in the other three cities.

The multifractal spectra of the shuffled and the surrogate hourly $PM_{2.5}$ and O_3 in four cities before and during the COVID-19 partial lockdown are shown in Figure 5 and the numerical results are shown in Table 2. The values of $\Delta\alpha_{x/y}$ show the apparent multifractality between the original $PM_{2.5}$ and O_3 series. The values of $\Delta\alpha^{shuf}_{x/y}$ are apparent multifractality between the shuffled series. The values of $\Delta\alpha^{surr}_{x/y}$ show the multifractality between the surrogate series. $\Delta\alpha^{SH,shuf}_{x/y,bl} = 0.112 \pm 0.062$ shows that the mean of the multifractality between shuffled $PM_{2.5}$ and O_3 in Shanghai before the COVID-19 lockdown, $\mathbb{E}(\Delta\alpha^{SH,shuf}_{x/y,bl})$, is 0.112 and the standard deviation of the multifractality between shuffled series, $STD(\Delta\alpha^{SH,shuf}_{x/y,bl})$, is 0.062. $\Delta\alpha^{SH,surr}_{x/y,bl} = 0.349 \pm 0.132$ shows that the mean of the multifractality between surrogate $PM_{2.5}$ and O_3 in Shanghai before the COVID-19 lockdown, $\mathbb{E}(\Delta\alpha^{SH,surr}_{x/y,bl})$, is 0.349 and the standard deviation of the multifractality between surrogate series, $STD(\Delta\alpha^{SH,surr}_{x/y,bl})$, is 0.132.

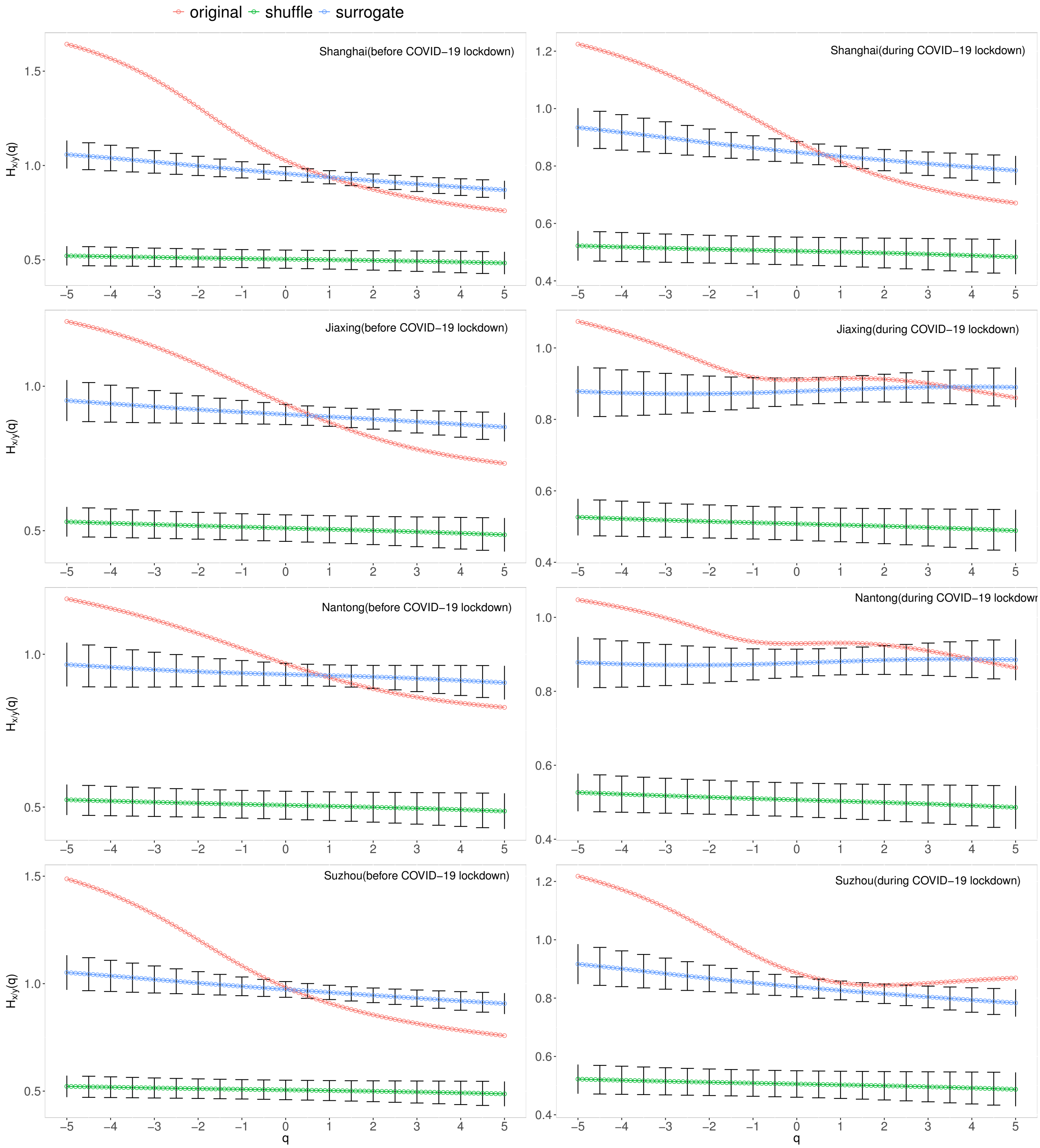

Figure 4. The q dependences of the generalized Hurst exponents $H_{x/y}(q)$ between the shuffled and surrogate hourly $PM_{2.5}$ and O_3 series in and around Shanghai before and during the COVID-19 partial lockdown. The error bars are the standard deviations for the 10,000 shuffled and surrogate series, respectively. "Original" is the MF-DCCA analysis result of the original $PM_{2.5}$ and O_3 series, "Shuffle" and "Surrogate" represent the MCASS analysis results of specified series obtained from shuffling and phase-randomizing the original series.

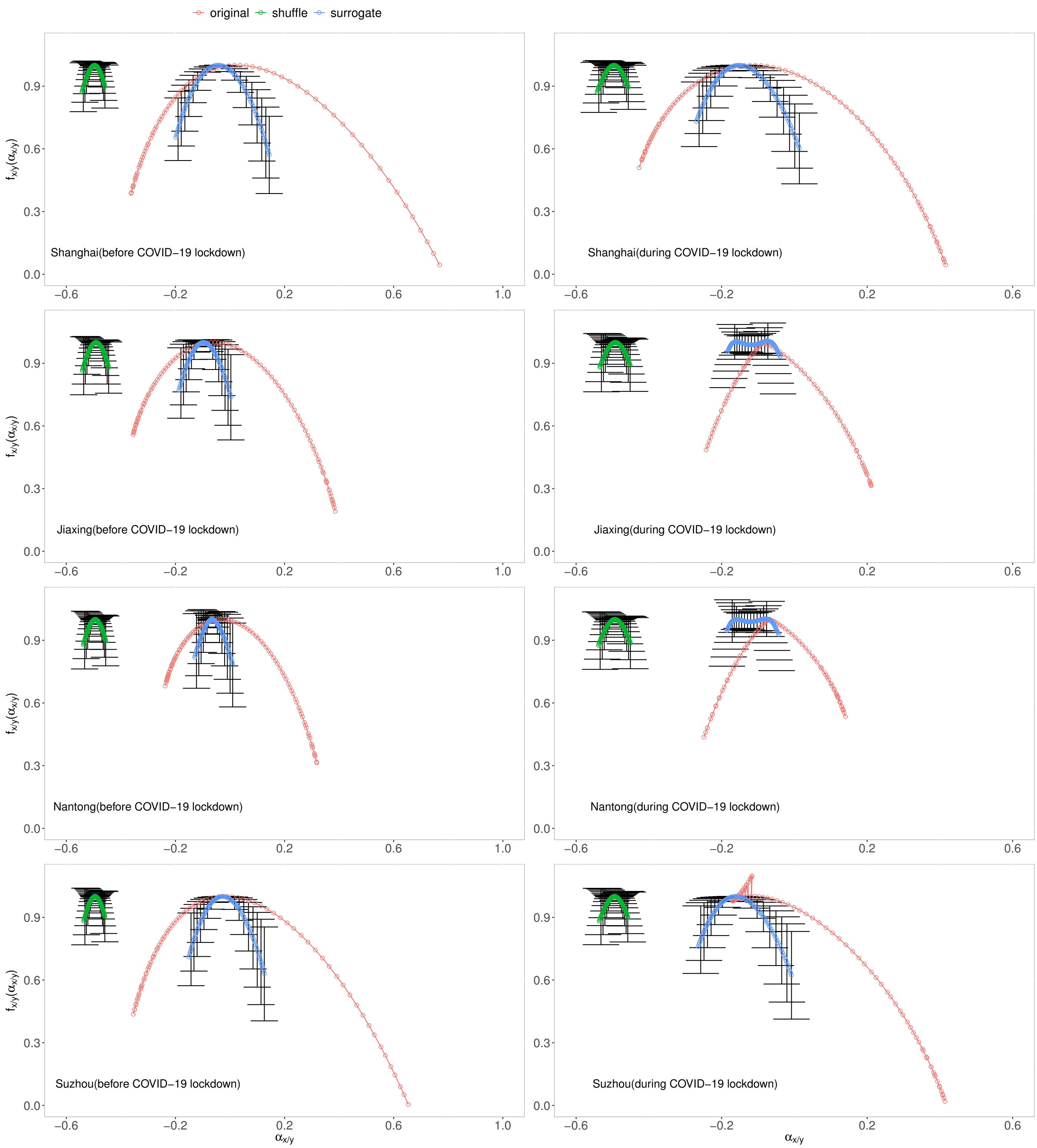

Figure 5. The multifractal spectra $(\alpha_{x/y}, f_{x/y}(\alpha_{x/y}))$ calculated from MCASS method between the shuffled and surrogate $PM_{2.5}$ and O_3 series in and around Shanghai before and during the COVID-19 partial lockdown. The error bars are the standard deviations for the 10,000 shuffled and surrogate series, respectively. "Original" is the MFDCCA analysis result of the original $PM_{2.5}$ and O_3 series, "Shuffle" and "Surrogate" represent the MCASS analysis results of specified series obtained from shuffling and phase-randomizing the original series.

Table 2. Comparison of the width of multifractal spectrums of original, shuffled, surrogate $PM_{2.5}$ and O_3 series in Shanghai, Jiaxing, Nantong and Suzhou before and during the COVID-19 partial lockdown. The numbers in parentheses are the standard deviations. Period I: before the COVID-19 lockdown, Period II: during the COVID-19 lockdown.

City	Pollutant	$\Delta\alpha_{x/y}$		$\Delta\alpha_{x/y}^{shuf}$		$\Delta\alpha_{x/y}^{surr}$	
		Period I	Period II	Period I	Period II	Period I	Period II
Shanghai	$PM_{2.5}$-O_3	1.321	0.843	0.112 (0.062)	0.115 (0.064)	0.349 (0.132)	0.292 (0.122)
Jiaxing	$PM_{2.5}$-O_3	0.741	0.454	0.125 (0.071)	0.119 (0.067)	0.218 (0.112)	0.145 (0.084)
Nantong	$PM_{2.5}$-O_3	0.556	0.389	0.116 (0.066)	0.120 (0.082)	0.189 (0.103)	0.142 (0.082)
Suzhou	$PM_{2.5}$-O_3	1.146	0.583	0.113 (0.066)	0.113 (0.123)	0.292 (0.135)	0.269 (0.123)

Based on Equations (8) and (10)–(12), the multifractal components between $PM_{2.5}$ and O_3 in Shanghai, Jiaxing, Nantong and Suzhou before and during the COVID-19 partial lockdown can be calculated and the results are illustrated in Table 3. The values of $\Delta\alpha_{x/y}^{LM}$ show the linear correlation multifractality. The values of $\Delta\alpha_{x/y}^{PDF}$ are the fat-tailed probability distribution multifractality. The values of $\Delta\alpha_{x/y}^{NL}$ show the nonlinear correlation multifractality. The values of $\Delta\alpha_{x/y}^{INTR}$ are the intrinsic multifractality part. The values of INTR $\text{ratio}_{x/y}$ are the ratio of the intrinsic multifractality to apparent multifractality. The multifractal components between $PM_{2.5}$ and O_3 in Shanghai before the COVID-19 partial lockdown can be obtained: $\Delta\alpha_{x/y,bl}^{SH,LM} = 0.237 \pm 0.146$ shows that the mean of the linear correlation multifractality, $\mathbb{E}(\Delta\alpha_{x/y,bl}^{SH,LM})$, is 0.237 and the standard deviation of the linear correlation part, $STD(\Delta\alpha_{x/y,bl}^{SH,LM})$, is 0.146, $\Delta\alpha_{x/y,bl}^{SH,PDF} = 0.112 \pm 0.062$, $\Delta\alpha_{x/y,bl}^{SH,NL} = 0.972 \pm 0.132$. The intrinsic multifractal cross-correlation is $\Delta\alpha_{x/y,bl}^{SH,INTR} = 0.972 \pm 0.132$.

Table 3. Comparison of the components of the width of multifractal spectrums of original, shuffled, surrogate $PM_{2.5}$ and O_3 series in and around Shanghai before and during the COVID-19 partial lockdown. The numbers in parentheses are the standard deviations. Period I: before the COVID-19 lockdown, Period II: during the COVID-19 lockdown.

City	Pollutant	$\Delta\alpha_{x/y}^{LM}$		$\Delta\alpha_{x/y}^{NL}$		$\Delta\alpha_{x/y}^{PDF}$		$\Delta\alpha_{x/y}^{INTR}$		INTR $\text{Ratio}_{x/y}$	
		Period I	Period II	Period I	Period II	Period I	Period II	Period I	Period II	Period I	Period II
Shanghai	$PM_{2.5}$-O_3	0.237 (0.146)	0.177 (0.138)	0.972 (0.132)	0.550 (0.122)	0.112 (0.062)	0.115 (0.064)	0.972 (0.132)	0.550 (0.122)	73.59% (9.98%)	65.32% (14.46%)
Jiaxing	$PM_{2.5}$-O_3	0.093 (0.132)	0.026 (0.108)	0.523 (0.112)	0.309 (0.084)	0.125 (0.071)	0.119 (0.067)	0.523 (0.112)	0.309 (0.084)	70.58% (15.10%)	68.16% (18.60%)
Nantong	$PM_{2.5}$-O_3	0.073 (0.122)	0.023 (0.106)	0.368 (0.103)	0.247 (0.082)	0.116 (0.066)	0.120 (0.082)	0.368 (0.103)	0.247 (0.082)	66.10% (18.49%)	63.41% (20.94%)
Suzhou	$PM_{2.5}$-O_3	0.179 (0.149)	0.156 (0.138)	0.854 (0.135)	0.314 (0.123)	0.113 (0.066)	0.113 (0.123)	0.854 (0.135)	0.314 (0.123)	74.53% (11.74%)	53.86% (21.01%)

Table 3 shows that the percentages of the intrinsic multifractality before and during the COVID-19 partial lockdown occupy a larger proportion of the total multifractality. Therefore, it can be concluded that the impacts of multifractality between $PM_{2.5}$ and O_3 in and around Shanghai generated from the nonlinear correlation part is greater than the fat-tailed probability distribution and linear correlation multifractality.

$\mathbb{E}(\text{INTR ratio}^{SH}_{x/y,dl}) < \mathbb{E}(\text{INTR ratio}^{SH}_{x/y,bl})$, $\mathbb{E}(\text{INTR ratio}^{JX}_{x/y,dl}) < \mathbb{E}(\text{INTR ratio}^{JX}_{x/y,bl})$, $\mathbb{E}(\text{INTR ratio}^{NT}_{x/y,dl}) < \mathbb{E}(\text{INTR ratio}^{NT}_{x/y,bl})$ and $\mathbb{E}(\text{INTR ratio}^{SZ}_{x/y,dl}) < \mathbb{E}(\text{INTR ratio}^{SZ}_{x/y,bl})$ imply that the intrinsic multifractality between $PM_{2.5}$ and O_3 in all cities decreased during the COVID-19 partial lockdown.

4.3. The Coordinated Control Degree of $PM_{2.5}$-O_3

To determine the coordinated control degree of $PM_{2.5}$-O_3 in and around Shanghai before and during the COVID-19 partial lockdown quantitatively, the index ζ in four cities are calculated according to Equation (15). The results are illustrated in Figure 6.

Although $\mathbb{E}(\text{INTR ratio})_{x/y}$ and $\sqrt{\sigma_x \sigma_y}$ both decrease, $\sqrt{\sigma_x \sigma_y}$ may drop deeply during the COVID-19 partial lockdown. Figure 6 shows that the mean values of ζ in and around Shanghai all increase during the COVID-19 partial lockdown. It indicates that the $PM_{2.5}$-O_3 coordinated control degrees in all four cities become weaker. Among these four cities, the added value of ζ in Shanghai is the maximum. The added value of ζ in Suzhou is the minimum.

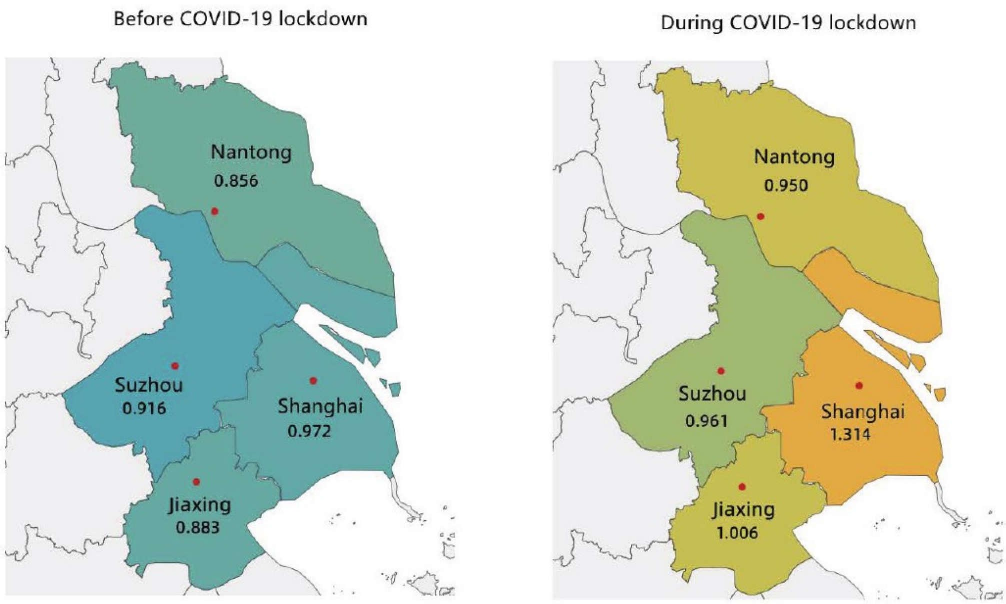

Figure 6. The mean values of ζ of $PM_{2.5}$-O_3 in Shanghai, Jiaxing, Nantong and Suzhou before and during the COVID-19 partial lockdown.

4.4. Disscussion

The nonlinear correlations are the genuine source of the multifractality [23,24], indicating the apparent multifractal cross-correlation may overestimate the multifractality of the series. The differences between change ratios in apparent and intrinsic multifractality are shown in Table 4.

Table 4. Comparison of the apparent ($\Delta\alpha_{x/y}$) and intrinsic ($\mathbb{E}(\text{INTR ratio})_{x/y}$) multifractal cross-correlation in and around Shanghai

City	Pollutant	$\Delta\alpha_{x/y}$			$\mathbb{E}(\text{INTR ratio})_{x/y}$		
		Period I(A)	Period II(B)	Change(B-A)/A	Period I(C)	Period II(D)	Change(D-C)
Shanghai	$PM_{2.5}$-O_3	1.321	0.843	−36.2%	73.59%	65.32%	−8.3%
Jiaxing	$PM_{2.5}$-O_3	0.741	0.454	−38.8%	70.58%)	68.16%	−2.4%
Nantong	$PM_{2.5}$-O_3	0.556	0.389	−30.0%	66.10%	63.41%	−2.7%
Suzhou	$PM_{2.5}$-O_3	1.146	0.583	−49.1%	74.53%	53.86%	−20.7%

The results suggest that although the COVID-19 lockdown contributes to the improvement of multifractal cross-correlations between $PM_{2.5}$ and O_3, their effects are limited from the perspective of intrinsic multifractality. Similar results are found in the effect of the COVID-19 control measures on the improvement of air quality. Almond et al. illustrated that air quality improved during the pandemic, but the improvement was smaller than expected, the reduction in SO_2 concentration was unobvious and the concentration of O_3 increased [30]. Zhao et al., reported that the concentrations of all pollutants except O_3 dropped in the initial period of the lockdown but rebounded with the resumption of work and production in later periods [31].

Among the four cities, the decreased percentage of intrinsic multifractality in Suzhou is the maximum. This may be the reason that causes the increased value of ζ in Suzhou to be minimum.

5. Conclusions

The outbreak of the COVID-19 pandemic caused serious restrictions on human activities in and around Shanghai. However, the period can be viewed as a helpful experiment to investigate the correlation between $PM_{2.5}$ and O_3 concentrations. In this paper, the dynamic impacts of the COVID-19 pandemic on the multifractal cross-correlations and the coordinated control degrees of $PM_{2.5}$-O_3 are examined. First of all, the multifractal cross-correlations, multifractality components and dynamic influences of the COVID-19 pandemic on cross-correlations between $PM_{2.5}$ and O_3 in four cities (i.e., Shanghai, Jiaxing, Nantong and Suzhou) are illustrated. Furthermore, a new quantification index, ζ, evaluating the coordinated control degree of $PM_{2.5}$-O_3 is developed, validated and compared. The main conclusions are as follows:

(1) The cross-correlations between $PM_{2.5}$ and O_3 in and around Shanghai both before and during the COVID-19 partial lockdown have multifractal characteristics. Moreover, there are weaker multifractal cross-correlation degrees of $PM_{2.5}$-O_3 in four cities during the COVID-19 partial lockdown.

(2) The impacts of multifractality due to the nonlinear correlation part in and around Shanghai are greater than the linear correlation part and the fat-tailed probability distribution part. The intrinsic multifractal cross-correlations between $PM_{2.5}$ and O_3 decreased in all cities during the COVID-19 partial lockdown.

(3) Although the COVID-19 lockdown contributes to the improvement of multifractal cross-correlations between $PM_{2.5}$ and O_3, their effects are limited from the perspective of intrinsic multifractality.

(4) The mean values of ζ in and around Shanghai all increased during the COVID-19 partial lockdown. This indicates that the $PM_{2.5}$-O_3 coordinated control degrees in all four cities become weaker. Among these four cities, the added value of ζ in Shanghai is the maximum.

Therefore, the dynamic impacts of the COVID-19 pandemic on the multifractal cross-correlations and the coordinated control degree of $PM_{2.5}$-O_3 provide new insights and a better understanding of the complex structure of $PM_{2.5}$-O_3. These findings help provide objective guidance for $PM_{2.5}$-O_3 coordinated control management. Due to the spatiotemporal difference in $PM_{2.5}$-O_3 coordinated control degree, each city should make different and specific strategies based on its requirements.

Author Contributions: Conceptualization, X.L.; methodology, X.L.; software, X.L.; validation, X.L. and F.S.; formal analysis, X.L.; investigation, X.L. and F.S.; data curation, X.L.; writing—original draft preparation, X.L.; writing—review and editing, X.L. and F.S.; visualization, X.L. All authors have read and agreed to the published version of the manuscript.

Funding: This research received no external funding.

Data Availability Statement: Not applicable.

Conflicts of Interest: The authors declare no conflict of interest.

References

1. Li, K.; Jacob, D.J.; Liao, H.; Zhu, J.; Shah, V.; Shen, L.; Bates, K.H.; Zhang, Q.; Zhai, S. A two-pollutant strategy for improving ozone and particulate air quality in china. *Nat. Geosci.* **2019**, *12*, 906–910. [CrossRef]
2. Wu, B.; Liu, C.; Zhang, J.; Du, J.; Shi, K. The multifractal evaluation of $PM_{2.5}$-O3 coordinated control capability in China. *Ecol. Indic.* **2021**, *129*, 107877. [CrossRef]
3. Wang, P.; Guo, H.; Hu, J.; Kot, S.H.; Ying, Q.; Zhang, H. Responses of $PM_{2.5}$ and O_3 concentrations to changes of meteorology and emissions in China. *Sci. Total. Environ.* **2019**, *662*, 297–306. [CrossRef] [PubMed]
4. Kroll, J.H.; Heald, C.L.; Cappa, C.D.; Farmer, D.K.; Fry, J.L.; Murphy, J.G.; Steiner, A.L. The complex chemical effects of COVID-19 shutdowns on air quality. *Nat. Chem.* **2020**, *12*, 777–779. [CrossRef] [PubMed]
5. Li, K.; Jacob, D.J.; Liao, H.; Shen, P.; Zhang, Q.; Bates, K.H. Anthropogenic drivers of 2013–2017 trends in summer surface ozone in China. *Proc. Natl. Acad. Sci. USA* **2019**, *116*, 422–427. [CrossRef]
6. Peng, C.K.; Buldyrev, S.V.; Havlin, S.; Simons, M.; Stanley, E.H.; Goldberger, A.L. Mosaic organization of DNA nucleotides. *Phys. Rev. E* **1994**, *49*, 1685–1689. [CrossRef]
7. Kantelhardt, J.W.; Zschiegner, S.A.; Koscielny-Bunde, E.; Havlind, S.; Bunde, A.; Stanley, H. Multifractal detrended fluctuation analysis of nonstationary time series. *Phys. A Stat. Mech. Its Appl.* **2002**, *316*, 87–114. [CrossRef]
8. Lee, C.K.; Juang, L.C.; Wang, C.C.; Liao, Y.Y.; Yu, C.C.; Liu, Y.C.; Ho, D.S. Scaling characteristics in ozone concentration time series (OCTS). *Chemosphere* **2006**, *62*, 934–946. [CrossRef]
9. Diosdado, A.M.; Coyt, G.G.; Lopez, J.B.; del Rio Correab, J. Multifractal analysis of air pollutants time series. *Rev. Mex. Fis.* **2013**, *59*, 7–13. [CrossRef]
10. Liu, Z.; Wang, L.; Zhu, H. Time–scaling property of air pollution indices: A case study of Shanghai, China. *Atmos. Pollut. Res.* **2015**, *6*, 886–892. [CrossRef]
11. Shen, C.; Huang, Y.; Yan, Y. An analysis of multifractal characteristics of API time series in Nanjing, China. *Phys. A Stat. Mech. Its Appl.* **2016**, *451*, 171–179. [CrossRef]
12. Dong, Q.; Wang, Y.; Li, P. Multifractal behavior of an air pollutant time series and the relevance to the predictability. *Environ. Pollut.* **2017**, *222*, 444–457. [CrossRef] [PubMed]
13. Wang, Q. Multifractal characterization of air polluted time series in China. *Phys. A Stat. Mech. Its Appl.* **2019**, *514*, 167–180. [CrossRef]
14. Li, X. On the multifractal analysis of air quality index time series before and during COVID-19 partial lockdown: A case study of Shanghai, China. *Phys. A Stat. Mech. Its Appl.* **2021**, *565*, 125551. [CrossRef]
15. Zhang, C.; Wang, X.; Chen, S.; Zou, L.; Zhang, X.; Tang, C. A study on daily $PM_{2.5}$ concentrations in Hong Kong using the EMD-based MFDFA method. *Phys. A Stat. Mech. Its Appl.* **2019**, *530*, 121182. [CrossRef]
16. Zhang, J.; Li, Y.; Liu, C.; Wu, B.; Shi, K. A study of cross-correlations between $PM_{2.5}$ and O_3 based on Copula and Multifractal methods. *Phys. A Stat. Mech. Its Appl.* **2022**, *589*, 126651. [CrossRef]
17. Zhou, W.X. Multifractal detrended cross-correlation analysis for two nonstationary signals. *Phys. Rev. E* **2008**, *77*, 066211. [CrossRef] [PubMed]
18. Xu, W.; Liu, C.; Shi, K.; Liu, Y. Multifractal detrended cross-correlation analysis on NO, NO_2 and O_3 concentrations at traffic sites. *Phys. A Stat. Mech. Its Appl.* **2018**, *502*, 605–612. [CrossRef]
19. Rak, R.; Grech, D. Quantitative approach to multifractality induced by correlations and broad distribution of data. *Phys. A Stat. Mech. Its Appl.* **2018**, *508*, 48–66. [CrossRef]
20. Bouchaud, J.P.; Potters, M.; Meyer, M. Apparent multifractality in financial time series. *Eur. Phys. J. B—Condens. Matter Complex Syst.* **2000**, *13*, 595–599. [CrossRef]
21. von Hardenberg, J.; Thieberger, R.; Provenzale, A. A box-counting red herring. *Phys. Lett. A* **2000**, *269*, 303–308. [CrossRef]
22. Saichev, A.; Sornette, D. Generic multifractality in exponentials of long memory processes. *Phys. Rev. E* **2006**, *74*, 011111. [CrossRef] [PubMed]
23. Drożdż, S.; Kwapień, J.; Oświecimka, P.; Rak, R. Quantitative features of multifractal subtleties in time series. *Europhys. Lett.* **2009**, *88*, 60003. [CrossRef]
24. Buonocorea, R.; Aste, T.; Matteo, T. Measuring multiscaling in financial time-series. *Chaos Solitons Fractals* **2016**, *88*, 38–47. [CrossRef]
25. Kwapień, J.; Oświecimka, P.; Drożdż, S. Components of multifractality in high-frequency stock returns. *Phys. A Stat. Mech. Its Appl.* **2005**, *350*, 466–474. [CrossRef]
26. Zhou, W.X. Finite-size effect and the components of multifractality in financial volatility. *Chaos Solitons Fractals* **2012**, *45*, 147–155. [CrossRef]
27. Jiang, Z.Q.; Xie, W.J.; Zhou, W.X.; Sornetted, D. Multifractal analysis of financial markets: A review. *Rep. Prog. Phys.* **2019**, *82*, 125901. [CrossRef] [PubMed]
28. Schreiber, T.; Schmitz, A. Improved Surrogate Data for Nonlinearity Tests. *Phys. Rev. Lett.* **1996**, *77*, 635. [CrossRef]
29. Chen, F.; Miao, Y.; Tian, K.; Ding, X.; Li, T. Multifractal cross-correlations between crude oil and tanker freight rate. *Phys. A Stat. Mech. Its Appl.* **2017**, *474*, 344–354. [CrossRef]

30. Almond, D.; Du, X.; Zhang, S. *Did COVID-19 Improve Air Quality Near HuBei?* National Bureau of Economic Research: Cambridge, MA, USA, 2020; No. W27086.
31. Zhao, X.; Shen, N.; Li, L.; Wu, J.; Tao, J.; Zhao, W. Analysis on changes and influencing factors of air pollutants in Beijing-Tianjin-Hebei region during COVID-19 epidemic. *Environ. Sci.* **2021**, *42*, 1–15.